A high-resolution simulation of convective roll clouds during a cold-air outbreak

A. Q. Liu
Department of Physics, University of Toronto, Toronto, Canada

G. W. K. Moore
Department of Physics, University of Toronto, Toronto, Canada

K. Tsuboki
Hydrospheric Atmospheric Research Center, Nagoya University, Nagoya, Japan

I. A. Renfrew
Physical Sciences Division, British Antarctic Survey, Cambridge, UK

Received 2 September 2003; revised 23 October 2003; accepted 25 November 2003; published 3 February 2004.

[1] A ubiquitous feature of the high latitude ocean is the occurrence of convective clouds that are organized into two-dimensional structures known as roll clouds or cloud streets. In this paper, we present a simulation of these structures that was performed in a domain large enough to simulate numerous roll clouds and their downstream evolution at a resolution sufficient to resolve the individual convective clouds. The simulations were initialized and validated using observations of roll clouds over the Labrador Sea. The model results indicate that the secondary flow associated with the roll clouds results in significant differences in the temperature, humidity and momentum fields between the updrafts and downdrafts. The model was also able to reproduce the observed downstream evolution of the clouds as the organization of the convection changed from two-dimensional rolls to three-dimensional closed cells. *INDEX TERMS:* 0320 Atmospheric Composition and Structure: Cloud physics and chemistry; 3210 Mathematical Geophysics: Modeling; 3307 Meteorology and Atmospheric Dynamics: Boundary layer processes. **Citation:** Liu, A. Q., G. W. K. Moore, K. Tsuboki, and I. A. Renfrew (2004) A high-resolution simulation of convective roll clouds during a cold-air outbreak, *Geophys. Res. Lett.*, *31*, L03101, doi:10.1029/2003GL018530.

1. Introduction

[2] Convective roll clouds are one of the most common forms of shallow boundary layer convection [*Etling and Brown*, 1993; *Atkinson and Zhang*, 1996]. They typically develop during cold-air outbreaks that are characterized by large air-sea temperature and humidity differences and high surface wind speeds. These characteristics provide favorable conditions for the development of convection that is organized into long quasi two-dimensional rolls. This organization results in cloud streets or roll clouds oriented along the direction of the mean low-level wind. Typically, the roll clouds are observed to evolve into cellular convection as one moves downstream from the coastline or ice edge. Figure 1 provides an example of the organization of the convection into cloud streets over the Labrador Sea [*Renfrew and Moore*, 1999]. Similar phenomena are observed over the Greenland Sea [*Hartmann et al.*, 1997], the Great Lakes [*Niziol et al.*, 1995] as well as over the Sea of Japan [*Tusboki et al.*, 1989].

[3] Theoretical, observational and modeling studies of roll clouds have been summarized by *Etling and Brown* [1993] and *Atkinson and Zhang* [1996]. These studies indicate that inflection point instability, parallel instability, and Rayleigh-Benard instability in the presence of vertical shear of the mean wind can all result in the development of roll clouds. During high latitude cold-air outbreaks, it appears that the first and the third mechanisms are most important, with no consensus as to which mechanism is most often dominant [*Brown*, 1972; *Hein and Brown*, 1988; *Moeng and Sullivan*, 1994; *Foster*, 1997; *Khanna and Brasseur*, 1998]. The detailed structure of roll clouds has been captured in field observations in a variety of locations [*Kristovich and Steve*, 1995; *Hartmann et al.*, 1997; *Brummer*, 1999; *Renfrew and Moore*, 1999]. These observations show a typical aspect ratio (ratio of roll wavelength to roll height) from 2 to 10. In addition, the aspect ratio typically increases downstream as rolls merge and evolve into cellular convection.

[4] Based on the observed homogeneity in the direction of the mean wind, roll clouds has been successfully simulated in several two-dimensional numerical models [*Mason and Sykes*, 1982; *Moeng*, 1984; *Coleman et al.*, 1994; *Hartmann et al.*, 1997]. However as a result of the absence

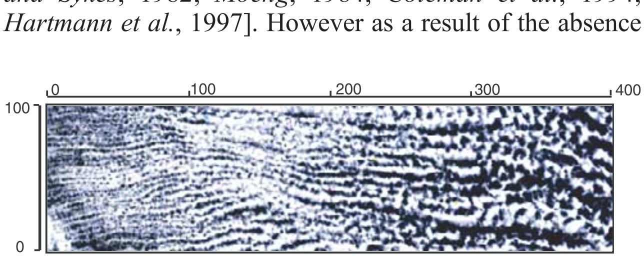

Figure 1. MODIS satellite image from 1525 UTC 12 April 1997 showing the development of cloud streets and cells associated with a cold air outbreak over the Labrador Sea. The extent of the domain is indicated in km.

0094-8276/04/2003GL018530$05.00

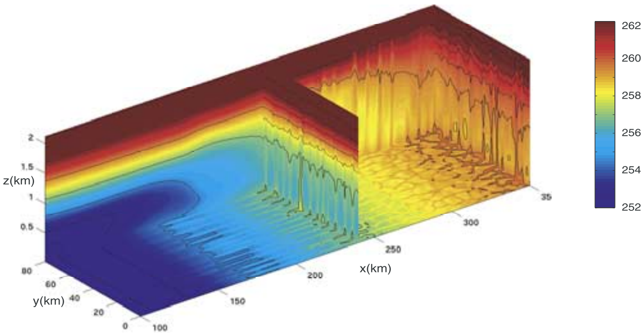

Figure 2. Three-dimensional display of the potential temperature field from the simulation at 10 hours. The x-z plane is at y = 80 km; the x-y plane is at z = 25 m; two y-z planes are at x = 240 km and x = 350 km separately.

of the third dimension, these models explicitly prohibit the development of structure in the direction of the mean wind and as a result cannot predict whether two-dimensional or three-dimensional convection should dominate the flow [*Atkinson and Zhang*, 1996]. Roll clouds have recently been studied in several high-resolution three-dimensional models [*Rao and Agee*, 1996; *Weckwerth et al.*, 1997; *Cooper et al.*, 2000; *Tian et al.*, 2003]. However all these simulations were performed in relatively small domains that constrained the boundary layer development and secondary flow evolution due to computing resource limitations. In addition, small domain simulations in a frame of reference moving with the mean wind have been used to explore some aspects of the evolution of roll convection [*Muller and Chlond*, 1996; *Muller et al.*, 1999]. As pointed out by *Atkinson and Zhang* [1996], ‘‘Three-dimensional numerical models, with domains large enough to capture the meso-scale structures in their larger contexts and with spatial resolutions fine enough to capture the internal behavior of the rolls and cells, probably offer the best opportunity for elucidating the mechanisms.’’ This study represents the first contribution of this kind of high-resolution large domain cloud resolving simulation of roll convection.

2. Numerical Model

[5] The model used in this study is the Cloud Resolving Storm Simulator (CReSS) developed at Nagoya University [*Tsuboki and Sakakibara*, 2002]. CReSS uses the non-hydrostatic and compressible equations of motion and includes a 1.5 order turbulent kinetic energy (TKE) closure and a bulk method for cold rain. Prognostic variables are three-dimensional velocity components, perturbation pressure and potential temperature as well as the mixing ratio for water vapor, and five species of hydrometeors. Cloud resolving simulations in a large domain require significant computational resources. CReSS's ability to run efficiently in a parallel computing environment allows it to be used to perform such simulations [*Tsuboki and Sakakibara*, 2002].

[6] The model domain used in these simulations was 400 km in the along roll (x) direction, 80 km in the cross roll (y) direction and 12 km in the vertical (z) direction. The horizontal grid interval was 500 m as used in *Cooper et al.* [2000] and *Tian et al.* [2003]. In the vertical, grid stretching was applied with the interval varying from 25 m near the surface to approximately 1 km near the top of the domain. As a result, the domain used in this simulation had 800 $\times$ 160 $\times$ 60 grid points. The model was initialized with the Goose Bay sounding data from 12Z on 8 February 1997. At this time, a cold-air outbreak was occurring over the Labrador Sea, downstream of Goose Bay, and roll clouds were observed with an instrumented aircraft [*Renfrew and Moore*, 1999]. To represent the environment in which these clouds developed, the first 100 km of the domain in the x direction was specified to be land at a fixed temperature of 248 K, while the remaining 300 km was specified to be ocean with a fixed sea surface temperature of 276 K. This is representative of conditions in the region as observed by the research vessel *Knorr* on this date [*LabSea Group*, 1998]. The surface and initial conditions were homogeneous in the y direction. To simplify the simulations, a free slip boundary condition was applied at the surface. Fluxes of heat, moisture and momentum between the surface and the atmosphere were parameterized using a bulk formulation [*Louis*, 1979]. Periodic boundary conditions were applied in the y direction, while wave radiation boundary conditions were applied in the x direction.

3. Results

[7] In Figure 2, we present the three-dimensional structure of the potential temperature field at 10 hours. The figure shows a deepening boundary layer with a well-defined roll structure as one proceeds downstream along the axis of the mean wind. The surface air temperature varies from 252 K near the coast to 258 K downstream at x = 300 km. This indicates that intense air-sea interaction was occurring. Indeed, the maximum sensible and latent heat flux reached 320 Wm^{-2} and 170 Wm^{-2} respectively. Three different vertical transport mechanisms for this transfer of heat and moisture can be inferred from this figure. Near the coast, the transport appears to be homogeneous and is most

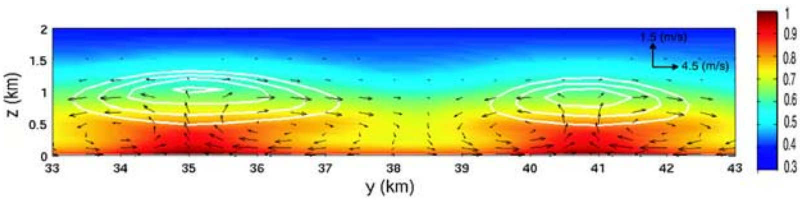

Figure 3. Detailed view of the secondary flow at x = 240 km associated with the roll convection at 10 hours. The specific humidity field (g kg^{-1}) is shaded, the cloud liquid water mixing ratio (g kg^{-1}) is contoured with contour interval 0.05 g kg^{-1} and the velocity (m s^{-1}) in the y-z plane is indicated by the vectors.

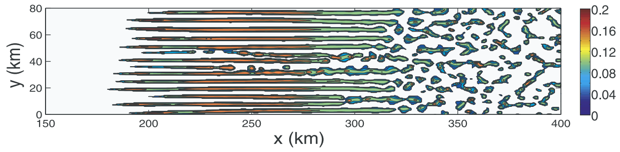

Figure 4. Horizontal cross-section of model simulated cloud mixing ratio field (g kg^{-1}) at z = 1 km and at 10 hours.

likely the result of subgrid-scale turbulence. Approximately 50 km from the coast (x = 150 km), convective rolls become dominant, while further downstream (x > 300 km) the rolls are replaced by cellular convection.

[8] A wavelength of around 4–6 km is representative of the modeled roll convection. The convective boundary layer (CBL) depth at x = 240 km is approximately 1.3 km resulting in an aspect ratio of about 3–5. On this date, the observed CBL depth at 150 km downstream from the ice zone was approximately 1.1 km and the observed roll wavelength was about 4–5 km, giving an aspect ratio of approximately 3.6–4.5 [*Renfrew and Moore*, 1999]. Hence there is good agreement between the model simulated roll structure and that observed.

[9] A close-up view of the structure of the rolls and their associated secondary flow is given in Figure 3, which shows a cross-section in the y-z plane at x = 240 km. The velocity field in this plane indicates that the updrafts are more intense and narrower than the downdrafts. The most intense upward motion of 1.5 m s^{-1} occurs at about 500 m height. The most humid air is located in the center of updrafts with a maximum value of 1 g kg^{-1}, while the driest air is between the rolls with a minimum humidity of about 0.7 g kg^{-1}. Again this is in good agreement with the observed humidity variations of 0.5 g kg^{-1} to 0.9 g kg^{-1} [*Renfrew and Moore*, 1999]. The cloud liquid water, shown in contours, indicates that cloud formed over the updrafts. There was also a combination of snowfall and graupel under the updrafts, with maximum rate of 1.2 mm h^{-1} (Snow Water Equivalent, SWE) for snowfall and 1.5 mm h^{-1} SWE for graupel. The strong inversion at the top of the boundary layer limits the vertical growth of the clouds and forces them to spread horizontally.

[10] The model simulated cloud liquid water mixing ratio field at 1 km height at 10 hours is shown in Figure 4. It clearly shows the transition from rolls to cells as one moves downstream over the ocean. Such transitions are often observed in nature [*Atkinson and Zhang*, 1996], but, to our knowledge, have never previously been fully captured in a numerical simulation.

[11] It is of interest to examine the mean flow changes that occurred in this simulation and the impact that they had on the organization of the convection. In Figure 5 we show vertical profiles of the potential temperature, specific humidity and zonal wind of the mean flow at the initial time and after 10 hours of model simulation at x = 240 km. Profiles at 10 hours are shown for both the updrafts and downdrafts. As was seen earlier, the figure shows the development of a well-mixed boundary layer reaching approximately 1 km in height. A comparison with the initial profiles indicates that the boundary layer becomes warmer and more humid. In addition, the updrafts are warmer and more humid than the downdrafts. With regard to the mean wind, the profiles indicate that the vertical shear in the boundary layer has been eliminated most likely through momentum mixing associated with the convection. In this respect, *Atkinson and Zhang* [1996] point out that roll convection tends to develop when the vertical wind shear is between 1 and 10 m s^{-1} km^{-1}, with cellular convection developing when the shear is less. Our results corroborate this observation, and suggest that the transition from roll to cellular convection is the result of the elimination of this shear by the secondary flow. Although the shear erosion is a gradual process as one moves downstream, the transition that results is relatively abrupt (Figures 2 and 4). Suggesting that the transition is being triggered by a modification in the mean flow that leads to a change in the nature of the convective instability affecting the flow.

4. Conclusions

[12] Boundary layer roll clouds as observed in high latitude cold-air outbreaks have been successfully simulated to develop out of a homogeneous initial state with a cloud resolving numerical model. We believe this is the first time that such a simulation has been performed at high enough resolution to explicitly resolve the convection and in a domain that is large enough to allow for the evolution of multiple cloud bands. The simulated secondary flow associated with the rolls leads to significant differences in the temperature, humidity and momentum fields between roll updrafts and downdrafts. These humidity variations, as well as the roll wavelength and aspect ratio, are all in good agreement with field observations. The model successfully reproduces the transition of the convection from rolls into closed cells as the vertical shear of zonal wind is eliminated through momentum mixing associated with the secondary

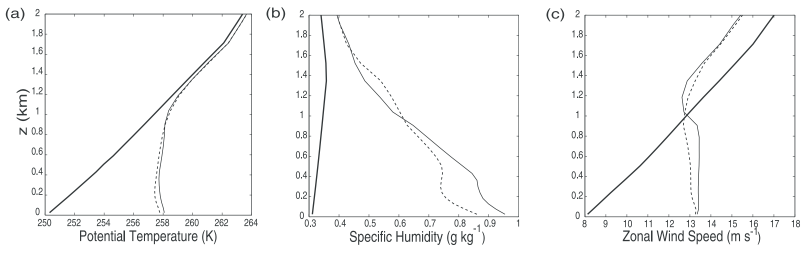

Figure 5. The evolution of vertical profiles of (a) potential temperature (K), (b) specific humidity (g kg^{-1}) and (c) zonal wind of the mean flow (m s^{-1}) at the initial time (thick solid line) and after 10 hours of model simulation at x = 240 km. Profiles at 10 hours are shown for the updrafts (thin solid line) and downdrafts (dashed line) separately.

flow; a process that is not available in two-dimensional models of roll convection. This work emphasizes the important role that parallel computing technology plays in our ability to realistically model organized convection in the atmosphere.

[13] **Acknowledgments.** This research was supported by the Canadian Foundation for Climate and Atmospheric Sciences. The authors would like to thank Mr. Atsushi Sakakibara for his assistance in developing CReSS. The simulations were performed on the NEC SX-6 supercomputer operated by the Atmospheric Physics group at the University of Toronto.

References

Atkinson, B. W., and J. W. Zhang (1996), Mesoscale shallow convection in the atmosphere, *Rev. Geophys.*, *34*(4), 403–431.

Brown, R. A. (1972), Inflection Point Instability of a Stratified Ekman Boundary-Layer, *J. Atmos. Sci.*, *29*(5), 984–986.

Brummer, B. (1999), Roll and cell convection in wintertime arctic cold-air outbreaks, *J. Atmos. Sci.*, *56*(15), 2613–2636.

Coleman, G. N., J. H. Ferziger, and P. R. Spalart (1994), A Numerical Study of the Convective Boundary-Layer, *Bound. -Layer Meteorol.*, *70*(3), 247–272.

Cooper, K. A., M. R. Hjelmfelt, R. G. Derickson, D. A. R. Kristovich, and N. F. Laird (2000), Numerical simulation of transitions in boundary layer convective structures in a lake-effect snow event, *Mon. Weather Rev.*, *128*(9), 3283–3295.

Etling, D., and R. A. Brown (1993), Roll Vortices in the Planetary Boundary-Layer — a Review, *Bound. -Layer Meteorol.*, *65*(3), 215–248.

Foster, R. C. (1997), Structure and energetics of optimal Ekman layer perturbations, *J. Fluid Mech.*, *333*, 97–123.

Hartmann, J., C. Kottmeier, and S. Raasch (1997), Roll vortices and boundary-layer development during a cold air outbreak, *Bound. -Layer Meteorol.*, *84*(1), 45–65.

Hein, P. F., and R. A. Brown (1988), Observations of Longitudinal Roll Vortices During Arctic Cold Air Outbreaks over Open Water, *Bound. -Layer Meteorol.*, *45*(1–2), 177–199.

Khanna, S., and J. G. Brasseur (1998), Three-dimensional buoyancy- and shear-induced local structure of the atmospheric boundary layer, *J. Atmos. Sci.*, *55*(5), 710–743.

Kristovich, D. A. R., and R. A. Steve (1995), A Satellite Study of Cloud-Band Frequencies over the Great- Lakes, *J. Appl. Meteorol.*, *34*(9), 2083–2090.

LabSea Group (1998), The Labrador Sea Deep Convection Experiment., *Bull. Am. Meteorol. Soc.*, *79*, 2033–2058.

Louis, J. F. (1979), Parametric Model of Vertical Eddy Fluxes in the Atmosphere, *Bound. -Layer Meteorol.*, *17*(2), 187–202.

Mason, P. J., and R. I. Sykes (1982), A Two-Dimensional Numerical Study of Horizontal Roll Vortices in an Inversion Capped Planetary Boundary-Layer, *Q. J. R. Meteorol. Soc.*, *108*(458), 801–823.

Moeng, C. H. (1984), A Large-Eddy-Simulation Model for the Study of Planetary Boundary-Layer Turbulence, *J. Atmos. Sci.*, *41*(13), 2052–2062.

Moeng, C. H., and P. P. Sullivan (1994), A Comparison of Shear-Driven and Buoyancy-Driven Planetary Boundary-Layer Flows, *J. Atmos. Sci.*, *51*(7), 999–1022.

Muller, G., and A. Chlond (1996), Three-dimensional numerical study of cell broadening during cold-air outbreaks, *Bound. -Layer Meteorol.*, *81*(3–4), 289–323.

Muller, G., B. Brummer, and W. Alpers (1999), Roll convection within an Arctic cold-air outbreak: Interpretation of in situ aircraft measurements and spaceborne SAR imagery by a three-dimensional atmospheric model, *Mon. Weather Rev.*, *127*(3), 363–380.

Niziol, T. A., W. R. Snyder, and J. S. Waldstreicher (1995), Winter Weather Forecasting Throughout the Eastern United-States. 4. Lake Effect Snow, *Weather and Forecasting*, *10*(1), 61–77.

Rao, G. S., and E. M. Agee (1996), Large eddy simulation of turbulent flow in a marine convective boundary layer with snow, *J. Atmos. Sci.*, *53*(1), 86–100.

Renfrew, I. A., and G. W. K. Moore (1999), An extreme cold-air outbreak over the Labrador Sea: Roll vortices and air-sea interaction, *Mon. Weather Rev.*, *127*(10), 2379–2394.

Tian, W. S., D. J. Parker, and C. A. D. Kilburn (2003), Observations and numerical simulation of atmospheric cellular convection over mesoscale topography, *Mon. Weather Rev.*, *131*(1), 222–235.

Tsuboki, K., and A. Sakakibara (2002), Large-scale Parallel Computing of Cloud Resolving Storm Simulator, in *High performance computing*, edited by P. Z. Hans, K. Joe, M. Sato, Y. Seo, and M. Schimasaki, pp. 564, Springer, Berlin.

Tusboki, K., Y. Fujiyoshi, and G. Wakahama (1989), Structure of Land Breeze and Snowfall Enhancement at the Leading Edge, *J. Meteorological Soc. of Japan*, *67*(5), 757–770.

Weckwerth, T. M., J. W. Wilson, R. M. Wakimoto, and N. A. Crook (1997), Horizontal convective rolls: Determining the environmental conditions supporting their existence and characteristics, *Mon. Weather Rev.*, *125*(4), 505–526.

A. Q. Liu and G. W. K. Moore, Department of Physics, University of Toronto, Toronto, Canada. (liuqi@atmosp.physics.utoronto.ca)

K. Tsuboki, Hydrospheric Atmospheric Research Center, Nagoya University, Nagoya, Japan.

I. A. Renfrew, Physical Sciences Division, British Antarctic Survey, Cambridge, U.K.